Title
Design of an advanced plasma chamber for third generation ECRIS

Journal
Review of Scientific Instruments, 96(6)

ISSN
0034-6748

Authors
Cruz-Duran, J
Benitez, JY
Garcia, JP
et al.

Publication Date
2025-06-01

DOI
10.1063/5.0260096

Peer reviewed

RESEARCH ARTICLE | JUNE 11 2025

Design of an advanced plasma chamber for third generation ECRIS

J. Cruz-Duran; J. Y. Benitez; J. P. Garcia; M. Handemagnon; C. M. Lyneis; L. Phair; D. S. Todd; D. Z. Xie

Rev. Sci. Instrum. 96, 063504 (2025)
https://doi.org/10.1063/5.0260096

Review of
Scientific nstruments

ARTICLE

pubs.aip.org/aip/rsi

Design of an advanced plasma chamber for third generation ECRIS

Cite as: Rev. Sci. Instrum. 96, 063504 (2025); doi: 10.1063/5.0260096
Submitted: 22 January 2025 • ccepted: 23 May 2025 •
Published Online: 11 June 2025

J. Cruz-Duran,[1,a)] J. Y. Benitez,[1] J. P. Garcia,[1] M. Handemagnon,[2] C. M. Lyneis,[1] L. Phair,[1] D. S. Todd,[1] and D. Z. Xie[1]

FFILI TIONS

[1] Lawrence Berkeley National Laboratory, Berkeley, California 94720, USA
[2] CEA Paris-Saclay, Saclay, France

[a)] uthor to whom correspondence should be addressed: jcruzduran@lbl.gov

BSTR CT

Current high performing electron cyclotron resonance ion sources (ECRISs), such as versatile ECR for nuclear science, are limited in the generation of higher beam intensities and higher charge states by the design of the plasma chamber and its cooling capacity. Because of the potential to damage a chamber by losses of energetic electrons from the plasma, an ECRIS must be tuned sub-optimally to prevent the creation of very energetic electrons. As such, the plasma chamber acts as a key limiting factor to the production capabilities of an ECRIS. The effects of parameters such as the location of the "hotspot" in relation to the water-cooling channels, the material of the walls, and the convective factor are analyzed to assess their impact on the thermal performance of the ECRIS plasma chamber.

I. INTRODUCTION

The Versatile ECR for NUclear Science (VENUS) ion source at LBNL is the world's first superconducting electron cyclotron resonance (ECR) ion source optimized for 28 GHz operation. This advanced ion source operates based on the principle of electron cyclotron resonance, where the plasma is magnetically confined and electrons are heated using microwaves. VENUS enables the extraction of high-intensity beams of medium charge states or low-intensity beams of higher charge states. The ion beams extracted from VENUS are utilized for important experimental studies, such as superheavy element production[1] and radiation and space effects testing.[2] However, its performance is limited by the plasma chamber design and its cooling capacity, which restrict VENUS's ability to reach optimal operating conditions using high radio frequency power at certain magnetic field configurations, as discussed further below.

High-performance ECR ion sources such as VENUS use higher plasma-confining magnetic fields, and as the fields rise, so do plasma electron energies. This increase in electron energy exacerbates electron heating effects, leading to greater challenges in controlling these effects and minimizing damage to the plasma chamber. Due to the risk of damaging the plasma chamber with "hot" electrons, an electron cyclotron resonance ion source (ECRIS) is often tuned to avoid creating excessively energetic electrons. Consequently, the plasma chamber becomes a key limiting factor in the production capabilities of the ion source.

During the ionization process, electrons escape the plasma where the magnetic field is weakest,[3–5] striking the chamber walls and transferring energy there. These regions, known as "hot spots," are where the highest temperatures in the chamber are reached. There are a total of six hot spots on the plasma chamber walls—three spaced evenly in each hotspot plane, as shown in Figs. 1 and 2. These hot spots arise because of the cancellation between the fringe fields of the axially confining solenoids and the radially confining sextupole. The solenoid at the opposite end of the source from beam extraction is stronger, and therefore the cancellation is stronger at one hotspot plane, the fields are weaker there, and the damage is typically greater. In addition, if the plasma chamber is not perfectly centered within the magnetic field, only one hotspot may form due to the asymmetry of the configuration.

In addition to any asymmetry due to misalignment between the plasma chamber and the magnetic field, the shape of the magnetic field also has a role in potential plasma chamber damage. Figure 3 depicts the axial magnetic field configuration of VENUS, where B_{inj} (3–4 T) is the magnetic field at the source injection, B_{min} (0.5–0.8 T)

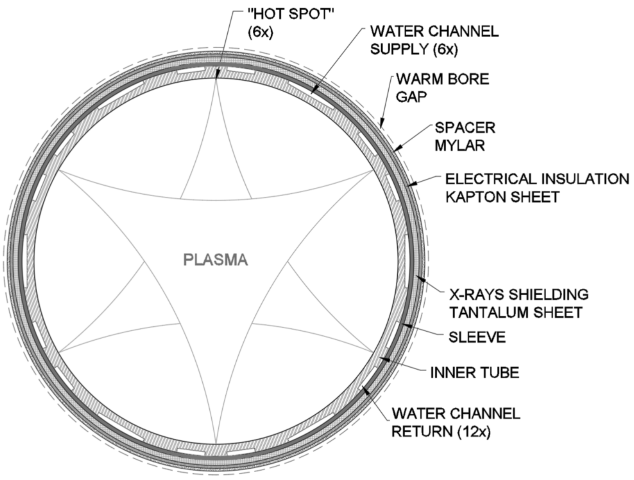

FIG. 1. Current VENUS plasma chamber design.

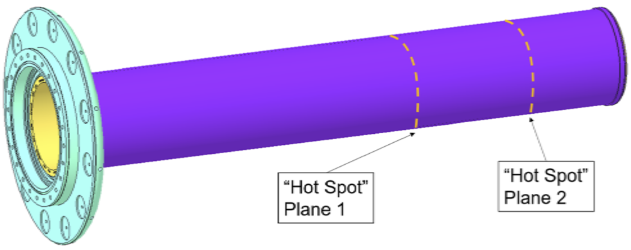

FIG. 2. VENUS plasma chamber "hotspot" location planes.

is the magnetic field in the center, and B_{ext} (2 T) is the magnetic field at the extraction.

The magnetic field configuration is crucial in the production of high-charge state ions. A higher minimum magnetic field (B_{min}), with respect to B_{ECR}, produces higher charge state ions. This is a result of the production of higher energy electrons at these high B_{min}

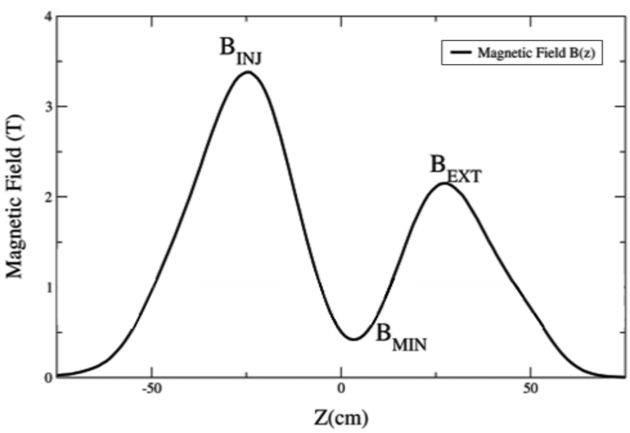

FIG. 3. An example of an axial magnetic field configuration for VENUS.

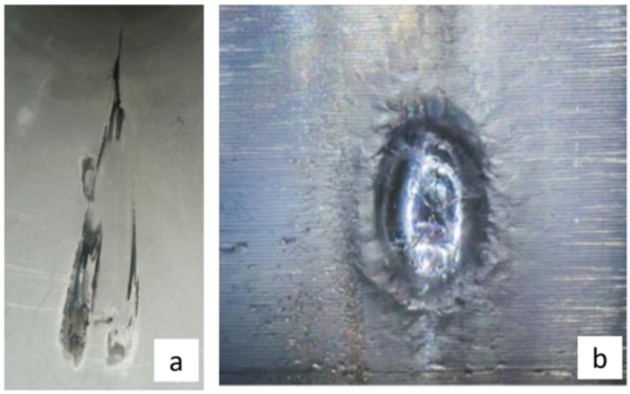

FIG. 4. Damage resulting from electron interaction with the plasma chamber walls. (a) Left: electrons are distributed, forming a flute shape. (b) Right: wall damage due to the effect of high B_{min}.

configurations. The B_{ECR} is the resonant magnetic field of the electrons that depends on radio frequency heating. For VENUS, using a resonance frequency of 28 GHz, B_{ECR} is 1 T.

Under the conditions where the ion source is operated at higher B_{min}, the electrons have more energetic interactions against the plasma chamber walls, causing damage as shown in Fig. 4.

The goal of this study is to explore ways to improve the VENUS plasma chamber's performance by enabling operation with higher B_{min}, which would increase electron energy and, in turn, allow for the production of higher charge state ions. This capability would significantly enhance the ion source's output and efficiency. The insights gained from this study will help improve the performance of current-generation ion sources, such as VENUS, and inform the development of future fourth generation sources, such as MARS.[6–8] These improvements include adjusting the locations of the hot spots in relation to the water cooling channels, selecting more appropriate materials for the chamber walls, and optimizing the convection coefficient. The convection coefficient represents the heat transfer from the solid surface to the fluid in contact with it per unit area and is influenced by the temperature difference between the solid and the fluid. It can be improved by increasing the fluid velocity and enhancing flow turbulence. In addition, the heat transfer can be improved by increasing the interface surface area between the solid and the fluid.

II. CURRENT VENUS PLASMA CHAMBER

The current VENUS plasma chamber is a cylindrical vessel composed of six pieces, as illustrated in Fig. 5. The primary material used in the design is Al 6061-T6.

The plasma chamber consists of two cylinders, which are slid over each other in a press-fit configuration. The inner cylinder serves as the structural master, incorporating milled cooling channels designed to cool the chamber walls. As electrons interact with the inner tube's wall, they deposit their energy.

The outer cylinder functions as the cap for the water-cooling channels. Wrapped around the cap are the electric insulation and the x-ray attenuator. Figure 1 depicts the layout of the plasma chamber,

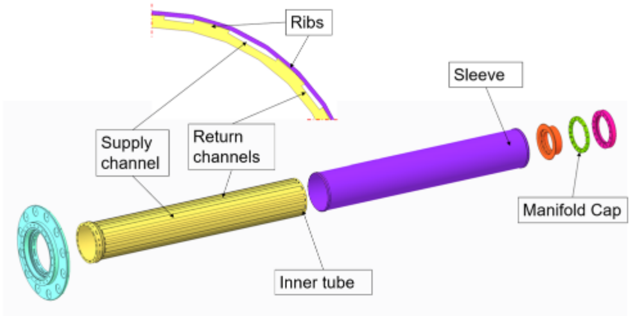

FIG. 5. VENUS plasma chamber main components.

along with the various insulators and shielding elements currently used in VENUS.

The plasma chamber is biased to a potential as high as 35 kV relative to the surrounding warm bore, necessitating the use of insulation between the two. Currently, three layers of 0.014 "thick Mylar and nine layers of 0.005" thick Kapton are used. The primary function of the Mylar layers is to center the plasma chamber within the warm bore.

III. CURRENT DESIGN SSESSMENT ND THERM L MODELING

A thermal analysis of the current VENUS plasma chamber was performed in ANSYS to evaluate the heat distribution and temperature behavior along the chamber walls. To simplify the study, only one of the hotspot planes shown in Fig. 2 was assessed, as the other was deemed sufficiently distant to have negligible thermal influence.

The hot spots were modeled as circular regions with a diameter of 4 mm, based on measurements from damaged plasma chambers. Each hotspot was assigned a thermal load of 400 W, estimated from the typical RF power level used during operation (8 kW) and accounting for 75% transmission losses between the RF system and the plasma chamber. It was assumed that 80% of the remaining power was deposited onto the cylindrical walls, with 50% of that concentrated in the hot-spot areas. The heat load was applied as a uniform distribution within each region; although a Gaussian profile would more accurately represent the actual power deposition, the uniform assumption is easier to implement and greatly shortens run-time when sweeping the many material, cooling, and geometry cases examined.

Applied uniformly over a 4 mm-diameter footprint, the 400 W load corresponds to 31.8 W mm ^{2}—yielding a higher local power density than an equivalent Gaussian profile and, thus, providing a conservative reference for evaluating the relative performance of different materials, cooling strategies, and chamber geometries.

A parametric convective heat transfer coefficient ranging from 100 to 100 000 W/m^2 K was applied to the circulating water flow, assuming an inlet temperature of 25 °C. While values up to 100 000 W/m^2 K were analyzed for completeness, achieving coefficients above 10 000–20 000 W/m^2 K is challenging in practice. However, reaching convective coefficients above 1000 W/m^2 K is generally

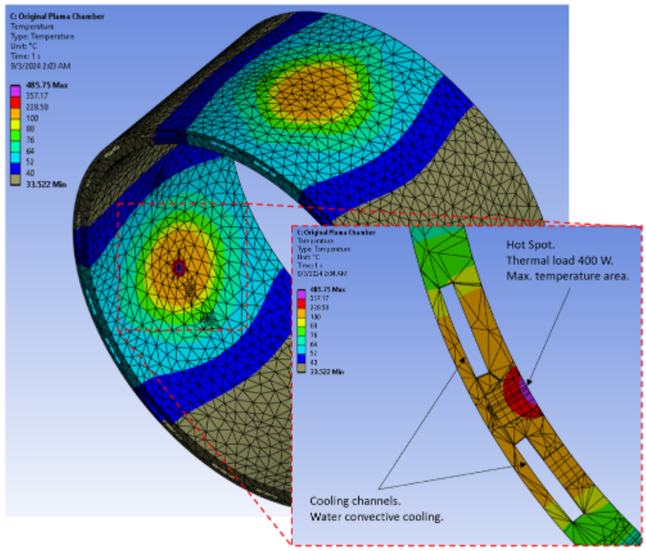

FIG. 6. VENUS plasma chamber thermal model. "Hotspot" between small (return) cooling channels.

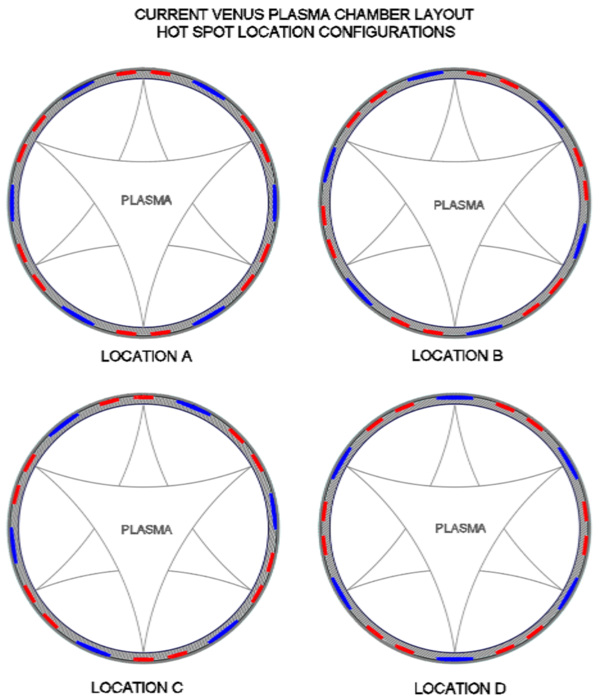

FIG. 7. Possible "hotspot" locations on the VENUS plasma chamber. Location A: between the small (return) channels; location B: between the big (supply) and small (return) channels; location C: on the small (return) channel; or location D: on the big (supply) channel. The supply and return channels are indicated in blue and red, respectively.

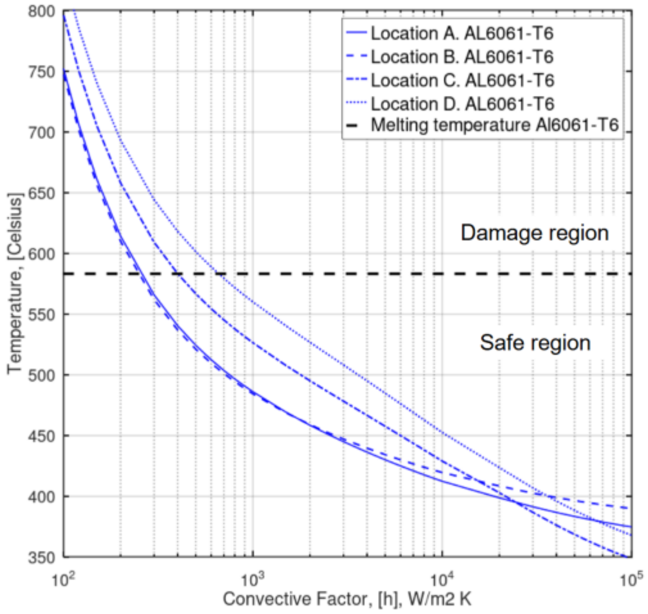

FIG. 8. Thermal model for different "hotspot" locations, as shown in Fig. 7, and convective coefficients.

feasible under standard cooling setups. Values near 100 000 W/m^2 K are considered theoretical and not attainable under typical operating conditions.

The key parameter to extract from the model is the maximum temperature reached in the location of the hotspot, as shown in Fig. 6. The plasma chamber can be rotated such that the "hot spots" can be aligned in four potential positions with respect to the water-cooling channels, as shown in Fig. 7.

As shown in Fig. 8, the location of the hotspot has a significant impact on wall temperature. When the convective coefficient is below 16 000 W/m^2 K, placing the hotspot on the ribs (locations A and B) results in lower temperatures and a greater margin to the material's melting point. In comparison, hot spots over the cooling channels (locations C and D) reach higher temperatures and operate closer to the melting limit throughout this range. At higher convective values, locating the hotspot over the channels becomes more effective in reducing temperature and increasing the thermal margin. However, such conditions are difficult to achieve in practice. In addition, when the hotspot is located on the ribs, increasing the convective coefficient beyond 10 000 W/m^2 K yields minimal temperature reduction, whereas hot spots over the channels continue to benefit from further convective enhancement.

IV. MATERIAL EFFECT

Other materials were assessed for the fabrication of the VENUS plasma chamber. The new materials studied were aluminum 6063-T6 and copper 11000-H10. These were selected based on the following criteria: thermal conductivity, melting temperature, mechanical properties such as yield and ultimate stress, material commercial availability, and manufacturability.

TABLE I. Thermal and mechanical properties of potential plasma chamber materials.

Properties/material	AL6061-T6	AL6063-T6	C11000-H10
Conductivity (W/m K)	167	200	380
Melting temperature (°C)	582	616	1084
Yield stress (MPa)	276	214	365
Ultimate stress (MPa)	310	241	395

The material properties from Table I show that changing the material from AL6061-T6 to AL6063-T6 or C11000-H10 has several advantages. The latter two materials have a higher melting temperature than the original one, which results in a higher safety factor before reaching melting. In addition, the materials have higher thermal conductivity, which implies that the heat can spread over a larger area, reducing the energy concentration over a narrow region.

The C11000-H10 material has superior mechanical properties, with higher yield and ultimate stress, compared to AL6061-T6.

On the other hand, the AL6063-T6 has slightly worse mechanical properties, such as ultimate and yield stress, than the AL6061-T6; although, since it is not a structural component and it is not under structural load, it should not be a limitation.

The change of the material from AL6061-T6 to AL6063-T6 in the plasma chamber would require a slight redesign due to the dimensions of the available stock material. However, the manufacturing process for this material would remain similar to the current one, which uses e-beam welding and TIG welding.

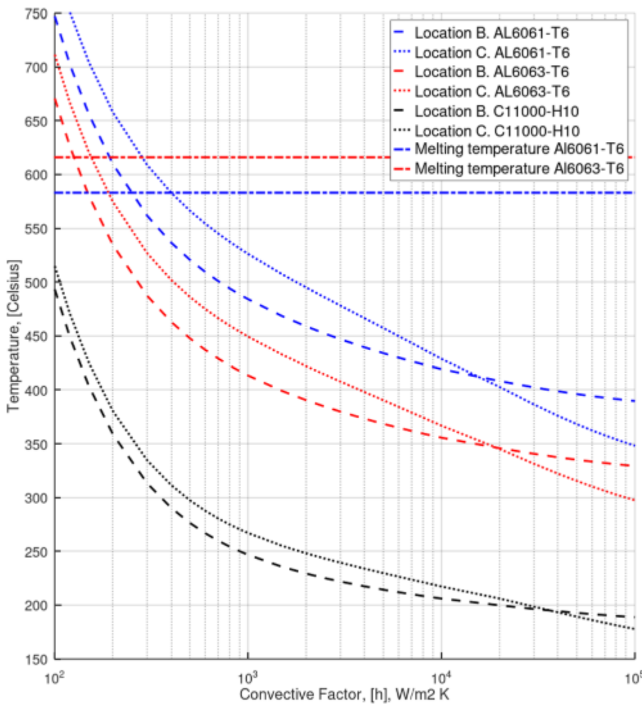

FIG. 9. "Hotspot" temperature for different materials and heat at locations B and C.

The use of C11000-H10 in the plasma chamber presents a known challenge: electron interaction with copper surfaces leads to copper sputtering and subsequent plasma poisoning. To prevent this, a thin layer of pure aluminum must be applied to the inner surface of the plasma chamber to act as a protective barrier. Developing a reliable coating process and ensuring its durability under operational conditions remain areas that require further research. In addition, the fabrication of a full copper chamber must be carefully assessed, particularly in terms of weldability, dimensional tolerances, and compatibility with existing manufacturing techniques.

From Fig. 9, we can conclude that improving the thermal conductivity of the chamber material significantly reduces the peak temperature at the "hotspot." A material with higher thermal conductivity distributes heat more effectively, preventing localized heat. The use of AL6063-T6 over AL6061-T6 provides an improvement factor of 1.23 at a convective coefficient of 1000 W/m^2 K, while C11000-H10 shows a much greater reduction, with an improvement factor of 3.52 for the same conditions.

Furthermore, it is observed that as the material's conductivity increases, the effectiveness of raising the convective coefficient becomes less pronounced. In other words, materials with better heat conduction require lower convective coefficients to reach the same target temperature. This implies that by optimizing the material, the thermal performance of the plasma chamber can be significantly enhanced while simultaneously reducing the operational demands on the cooling system.

V. W TER CH NNEL GEOMETRY

The new proposed layout eliminates the Mylar layer previously used to center the plasma chamber within the warm bore of the ECR ion source, thereby increasing the available space and allowing the radius of the inner tube to expand by 0.042 in., as shown in Fig. 10. This modification enables an increase in the length, height, and area of the cooling channels, which is intended to enhance water flow and improve heat removal. The inner diameter of the plasma chamber remains fixed, as the radial magnetic field scales with the square of the radius. A reduction in this dimension would lower the magnetic field strength and compromise the ionization efficiency of the source.

In the context of this new layout, different cooling channel configurations were analyzed to evaluate the thermal behavior and its impact on the hotspot temperature. A significant design change in the new layout involves reducing the number of cooling channels from 18 to 12. This is accomplished by switching from two return channels per supply to a single, larger return, with the goal of simplifying flow paths and improving overall fluid flow.

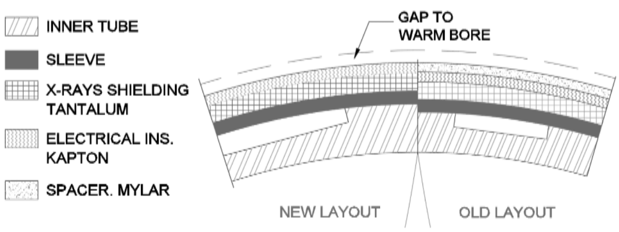

FIG. 10. VENUS plasma chamber. New (left) vs old layout (right).

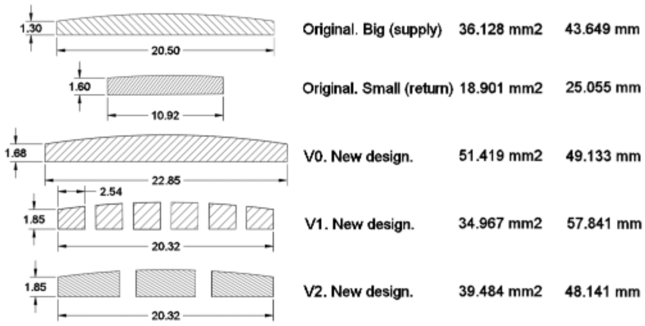

FIG. 11. VENUS plasma chamber. Original and proposed cooling channels. Shaded areas represent the channel cross section; this value is expressed in the table in mm^2 in the central column. In the right column, the total perimeter of the channel in mm is expressed.

Three alternative geometries—V0, V1, and V2—were developed based on the updated chamber layout and are shown in Fig. 11. Geometry V0 features a single, larger flow channel relative to the original configuration. V1 and V2 explore the addition of fins within the channels to evaluate how increased internal surface area affects thermal performance. Notably, V1 is similar to the microchannel solution adopted in Ref. 3, which demonstrated improved thermal behavior in high-power ECR ion sources.

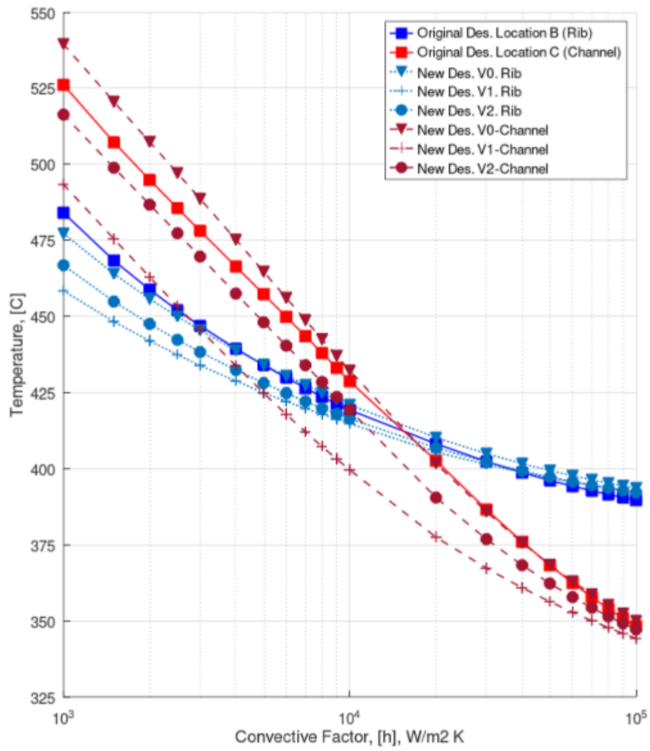

FIG. 12. "Hotspot" temperature. Old vs new plasma chamber layout for different channel designs. Aluminum 6061-T6.

Figure 12 shows the hotspot temperatures for the original design at locations B and C, which serve as baselines for comparison with the new geometries. For each new configuration (V0 to V2), the hotspot was placed both over the rib and over the channel to evaluate thermal performance under varying heat load conditions. The results indicate that increasing the number of fins reduces the hotspot temperature in both scenarios.

When the hotspot is located over the rib, the thermal response is less sensitive to variations in the convective heat transfer coefficient. In this case, the temperature tends to plateau beyond 10 000 W/m^2 K, indicating limited benefit from further increases in convection. In contrast, when the hotspot is placed over the channel, the temperature decreases more steadily as convection increases, with the plateau occurring at higher convective values. At low convective coefficients, the hotspot over the channel exhibits higher peak temperatures than when located over the rib.

However, for microchannel configurations with high fin density (V1), the thermal performance at 5000 W/m^2 K is similar regardless of whether the hotspot is over the rib or the channel. As the convective coefficient approaches the upper bound of the practical range—around 20 000 W/m^2 K—a moderate advantage emerges when the hotspot is located over the channel, with a temperature reduction of 30 °C compared to having it over the rib. While this represents a performance improvement, it is not substantial. Moreover, increasing the convective coefficient beyond this range is technically challenging and yields diminishing returns as the temperature approaches a plateau.

Therefore, within the practical operating range of 5000–20 000 W/m^2 K, microchannel designs with increased fin density offer some degree of temperature reduction when the hotspot is located over the channel, with a more gradual thermal saturation compared to rib-based configurations, which reach their plateau earlier.

Although finned or microchannel designs improve thermal performance by increasing the heat exchange surface, their implementation is constrained by practical considerations. These configurations introduce additional pressure drops, requiring higher water supply pressure, and are typically applicable only over limited sections of the channel to avoid excessive hydraulic losses. As a result, the thermal gains provided by microchannel geometries must be weighed against these operational trade-offs.

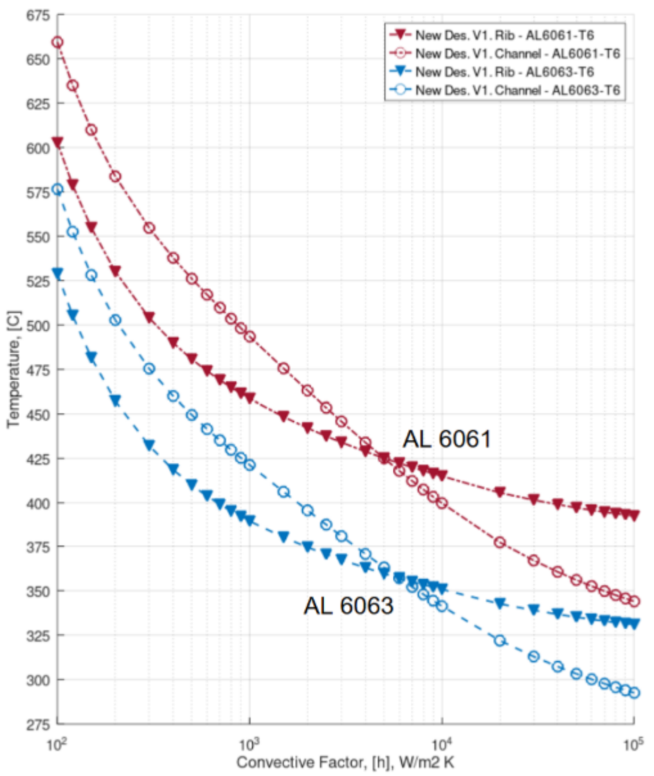

FIG. 13. Plasma chamber peak temperature for different materials, "hotspot" locations, and convection factors.

VI. EV LU TION OF TEMPER TURE REDUCTION STR TEGIES

Figure 13 shows the peak temperature of the plasma chamber using geometry V1, evaluated for AL6061 and AL6063 across a range of convective coefficients and hotspot locations (over the rib and over the channel). This configuration is used exclusively in the final comparison, as Sec. V demonstrated that V1 outperforms the original geometry—particularly at low convection—with minimal differences at higher values. The results confirm that AL6063 consistently achieves lower hotspot temperatures than AL6061, regardless of load location or convection level.

VII. CONCLUSIONS

Improving the thermal performance of ECR ion sources depends largely on the thermal conductivity of the plasma chamber material. Aluminum 6063-T6 performs better than the current 6061-T6 alloy, consistently lowering peak temperatures across all conditions.

Placing the hotspot over the channels can lead to local boiling when surface temperatures exceed 165 °C (the boiling point of water at 100 psi pressure), forming vapor pockets that reduce convective efficiency.[3,4] This occurs when the convective heat transfer coefficient is too low to prevent phase change at the surface.

While microchannel designs enhance cooling by increasing surface area, material thermal conductivity has a stronger impact on reducing hotspot temperatures. The best solution combines high-conductivity materials with microchannel geometries, achieving more effective and reliable thermal management.

CKNOWLEDGMENTS

This work was supported by royalties received by the Engineering Division from the licensing of laboratory intellectual property by the division's inventors.

UTHOR DECL R TIONS

Conflict of Interest

The authors have no conflicts to disclose.

uthor Contributions

J. Cruz-Duran: Conceptualization (equal); Data curation (equal); Formal analysis (equal); Funding acquisition (equal); Investigation (equal); Methodology (equal); Project administration (equal); Resources (equal); Supervision (equal); Visualization (equal); Writing – original draft (equal); Writing – review & editing (equal). **J. Y. Benitez**: Conceptualization (equal); Funding acquisition (equal); Investigation (equal); Methodology (equal); Validation (equal); Writing – original draft (equal); Writing – review & editing (equal). **J. P. Garcia**: Conceptualization (equal); Investigation (equal); Methodology (equal). **M. Handemagnon**: Conceptualization (equal); Investigation (equal). **C. M. Lyneis**: Conceptualization (equal); Funding acquisition (equal); Investigation (equal); Resources (equal); Writing – original draft (equal). **L. Phair**: Conceptualization (equal); Funding acquisition (equal); Methodology (equal); Resources (equal); Writing – original draft (equal); Writing – review & editing (equal). **D. S. Todd**: Conceptualization (equal); Funding acquisition (equal); Methodology (equal); Writing – original draft (equal); Writing – review & editing (equal). **D. Z. Xie**: Conceptualization (equal); Funding acquisition (equal); Methodology (equal).

D T V IL BILITY

The data is available from the corresponding author upon request.

REFERENCES

[1] J. M. Gates, R. Orford, D. Rudolph *et al.*, "Toward the discovery of new elements: Production of livermorium (Z 116) with ^{50}Ti," Phys. Rev. Lett. **133**, 172502 (2024).
[2] J. Y. Benitez, A. Donoghue, M. B. Johnson, W. Lu, B. Ninemire, L. Phair, D. S. Todd, and D. Xie, "Recent cocktail beam developments at the 88-inch cyclotron for SEE testing," in *Proceedings of the 2017 IEEE Nuclear and Space Radiation Effects Conference (NSREC17)* (IEEE, New Orleans, LA, 2017), pp. 1–5.
[3] J. W. Guo, L. B. Li, J. D. Ma, L. X. Li, Y. C. Feng, W. Lu, W. H. Zhang, X. Fang, X. Z. Zhang, Y. Y. Yang, Y. J. Zhai, W. Huang, D. Hitz, L. T. Sun, and H. W. Zhao, "A new solution to plasma chamber cooling for high power ECR ion source operation," in *The 24th International Workshop on ECR Ion Source*, East Lansing, MI, 28–30 September 2020 (JACoW, 2020).
[4] T. Thuillier, J. Angot, J. Y. Benitez, A. Hodgkinson, C. M. Lyneis, D. S. Todd, and D. Z. Xie, "Investigation on the electron flux to the wall in the VENUS ion source," Rev. Sci. Instrum. **87**, 02A736 (2016).
[5] J. Benitez, C. Lyneis, L. Phair, D. Todd, and D. Xie, "Dependence of the bremsstrahlung spectral temperature in minimum-B electron cyclotron resonance ion sources," IEEE Trans. Plasma Sci. **45**(7), 1746 (2017).
[6] D. Z. Xie, "A new structure of superconducting magnetic system for 50 GHz operations (invited)," Rev. Sci. Instrum. **83**, 02A302 (2012).
[7] D. Z. Xie, J. Y. Benitez, A. Hodgkinson, T. Loew, C. M. Lyneis, L. Phair, P. Pipersky, B. Reynolds, and D. S. Todd, "Development status of a next generation ECRIS: MARS-D at LBNL," Rev. Sci. Instrum. **87**, 02A702 (2016).
[8] D. Z. Xie, J. Y. Benitez, A. Hodgkinson, T. Loew, C. M. Lyneis, L. Phair, P. Pipersky, B. Reynolds, and D. S. Todd, "Design of a new superconducting magnet system for high strength minimum-B fields for ECRIS," IEEE Trans. Appl. Supercond. **26**(4), 4100205 (2016).